Multiple Metamagnetic Quantum Criticality in Sr₃Ru₂O₇

Y. Tokiwa,[1,2] M. Mchalwat,[1] R. S. Perry,[3] and P. Gegenwart[1,4]

[1]*I. Physikalisches Institut, Georg-August-Universität Göttingen, 37077 Göttingen, Germany*
[2]*Department of Physics, Kyoto University, Kyoto 606-8502, Japan*
[3]*London Centre for Nanotechnology, Faculty of Maths & Physical Sciences, University College London,*
London–WC1E 6BT, United Kingdom
[4]*Experimentalphysik VI, Center for Electronic Correlations and Magnetism, Augsburg University,*
86159 Augsburg, Germany
(Received 23 February 2016; published 31 May 2016)

Bilayer strontium ruthenate $Sr_3Ru_2O_7$ displays pronounced non-Fermi liquid behavior at magnetic fields around 8 T, applied perpendicular to the ruthenate planes, which previously has been associated with an itinerant metamagnetic quantum critical end point (QCEP). We focus on the magnetic Grüneisen parameter Γ_H, which is the most direct probe to characterize field-induced quantum criticality. We confirm quantum critical scaling due to a putative two-dimensional QCEP near 7.845(5) T, which is masked by two ordered phases *A* and *B*, identified previously by neutron scattering. In addition, we find evidence for a QCEP at 7.53 (2) T and determine the quantum critical regimes of both instabilities and the effect of their superposition.

Quantum criticality denotes critical behavior that is associated with continuous transformations of matter at zero temperature. Because of the absence of thermal fluctuations at $T = 0$ it is qualitatively different from classical criticality [1]. In metals the unconventional excitation spectrum near a quantum critical point (QCP) causes the breakdown of Fermi liquid (FL) behavior and its intimate relation to exotic states, such as unconventional superconductivity, adds even more importance to this topic. To date, the influence of quantum critical magnetic excitations on electrons in a metal is far from being understood. For instance, the applicability of the itinerant Hertz-Millis-Moriya theory on f-electron-based Kondo lattice systems has been disproved by several experiments [2] and alternative descriptions are not fully established yet. Quantum criticality related to itinerant metamagnetism is exceptional in the sense that electronic degrees of freedom are irrelevant, and a quantitative application to experimental results should be possible [3].

The generic metamagnetic quantum critical end point (QCEP) arises from the suppression to $T = 0$ of the end point of a line of first-order metamagnetic transitions in temperature-field phase space by tuning, e.g., composition, pressure, or the magnetic field orientation [3]. Metamagnetic QCEPs have been realized in the f-electron-based compounds $CeRu_2Si_2$ [4,5] and $UCoAl$ [6], as well as d-electron $Sr_3Ru_2O_7$ [7,8].

We focus on bilayer strontium ruthenate $Sr_3Ru_2O_7$. Magnetization of this compound along the tetragonal c axis at low temperature exhibits three successive superlinear, i.e., metamagnetic, rises at $\mu_0 H_{M1} = 7.5$ T, $\mu_0 H_{M2} = 7.85$ T, and $\mu_0 H_{M3} = 8.1$ T [9]. The first one is a metamagnetic crossover ($M1$). The second and third ones are first-order metamagnetic transitions ($M2$ and $M3$), ending at critical

temperatures of about 1 and 0.5 K, respectively [10]. A line of second-order thermal phase transitions, connecting the critical end points of $M2$ and $M3$, has been discovered in electrical resistivity and thermodynamic experiments [10,11], which recently by neutron scattering has been identified as phase boundary of a spin-density-wave (SDW) "phase *A*" [12,13] (see Fig. 1.). The lower and upper critical fields of SDW-*A* correspond, respectively, to H_{M2} and H_{M3}. Additionally, another SDW "phase *B*" has been observed in between H_{M3} and 8.3 T [12,15]. The observed incommensurate ordering vectors in both SDW phases have been related to Fermi surface nesting [12]. Magnetic susceptibility and magnetostriction have revealed the strongest peak at the $M2$ metamagnetic transition and weaker maxima at $M1$ and $M3$ [10]. The critical field has been extrapolated to $\mu_0 H_{c2} = 7.845(5)$ T [11], which is indeed very close to $\mu_0 H_{M2}$. Non-Fermi-liquid behavior at elevated temperatures was previously associated with a critical field close to H_{M2} [9]. Outside the SDW phases *A* and *B* and not too close to the $M1$ crossover, thermal expansion obeys quantum critical scaling in accordance with the expectations for a two-dimensional (2D) metamagnetic QCEP near 7.845 T [11]. This includes both the predicted divergence upon cooling within the quantum critical regime as well as the magnetic field dependence within the low-temperature FL regime upon tuning the field from both sides towards $M2$. However, the previous description of the specific heat coefficient C/T by a strong divergence $|H_{M2} - H|^{-1}$ [8,16] is in clear contradiction to the theoretical prediction $C/T \sim |H_c - H|^{-1/3}$ [3].

We solve this discrepancy by proving that $Sr_3Ru_2O_7$ displays two QCEPs at $\mu_0 H_{c1} = 7.53(2)$ T and $\mu_0 H_{c2} = 7.845(5)$ T, respectively. We determine regimes in phase space where either of the two QCEPs leads to scaling of the
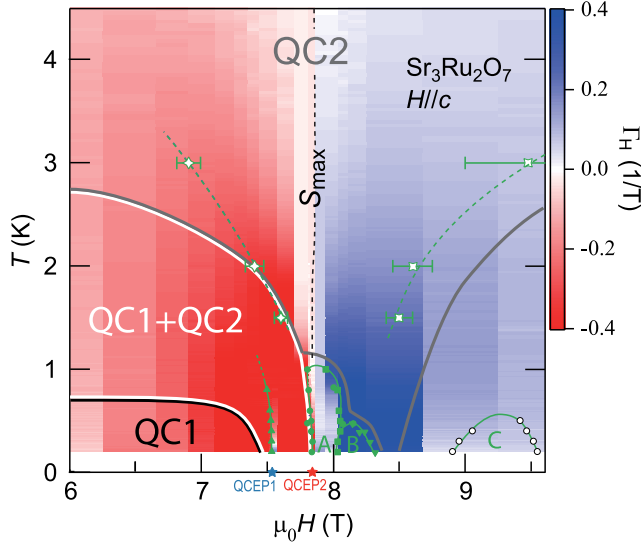
FIG. 1. Phase diagram of $Sr_3Ru_2O_7$ for $H\|c$ with color coding of the magnetic Grüneisen parameter Γ_H. Solid green symbols mark positions of sharp anomalies in $\Gamma_H(T,H)$, related to metamagnetism [10] and the spin-density-wave phases A and B [12]. Open green symbols indicate positions of maxima in the field dependence of specific heat. The dotted black line marks $\Gamma_H = 0$, corresponding to a local entropy maximum. The stars on the x axis show the positions of the two metamagnetic quantum critical end points QCEP1 and QCEP2. Gray, white, and black solid lines bound different regimes. Labels "QC1" and "QC2" denote regions where quantum critical scaling with respect to QCEP1 and QCEP2 is observed. Within the QC1 + QC2 regime, scaling fails due to the superposition of criticality from both instabilities, see Supplemental Material [14]. Anomalies in isothermal $\Gamma_H(H)$ scans are indicated as the yet unidentified regime "C".

magnetic Grüneisen parameter. We also show where scaling fails due to the superposition of criticality from both instabilities. Multiple quantum criticality as an origin for behavior that is incompatible with the generic predictions of QCPs can be of relevance for various material classes.

The magnetic Grüneisen parameter $\Gamma_H = T^{-1}(dT/dH)_S$ measures the relative temperature change with magnetic field under adiabatic conditions, called the adiabatic magnetocaloric effect. Because of the entropy accumulation near field-driven quantum criticality, generically this property is expected to obey (i) a sign change when tuning the field across the critical value, (ii) a divergence upon cooling (at constant field) within the quantum critical regime [17,18], and (iii) universal scaling within both the FL and quantum critical regime. The adiabatic magnetocaloric effect can be accurately determined with the aid of the alternating-field method [19]. Using this technique several field-induced quantum critical points have been characterized [20–22]. The magnetic Grüneisen parameter provides direct access to the critical exponents which characterize quantum criticality. Below, we report a thorough study of Γ_H, determined by the alternating-field technique [19], as

well as heat capacity measurements performed with the quasiadiabatic heat pulse technique, on a high-quality single crystal of $Sr_3Ru_2O_7$, grown by the floating zone technique [23], for fields applied along the c axis.

Figure 2 displays the magnetic field dependence of the specific heat coefficient at various low temperatures. Data at 0.2 K display a single peak at 7.85 T. At larger temperatures, this peak is split into two peaks and the respective separation increases with increasing temperature. Qualitatively, such behavior is characteristic of itinerant metamagnetism and has also been found for $CeRu_2Si_2$ [25]. For a generic QCEP with a critical free energy $F_{cr}(h) = F_{cr}(-h)$ [where $h = \mu_0(H - H_c)$], symmetric peaks for the heat capacity are expected. Our measurements, however, display more broadened C/T peaks on the high field compared to the low-field sides. As discussed later, this may be related to a slight increase of the effective dimensionality of the critical fluctuations at large fields.

The magnetic field dependence of the 0.2 K data is in perfect agreement with previous data [8,16], see Supplemental Material [14]. As shown by the blue solid line in Fig. 2, the data are well described by $C/T \propto (H_c - H)^{-1/3}$, predicted for a 2D QCEP [3,24] with critical field close to H_{M1} but significantly smaller than H_{M2}. This indicates that the previously anticipated scenario with a *single* field-tuned QCEP near H_{M2} [8] is insufficient.

The existence of two separate 2D metamagnetic QCEPs is evident from the analysis of the magnetic Grüneisen parameter Γ_H given below. In contrast to the specific heat
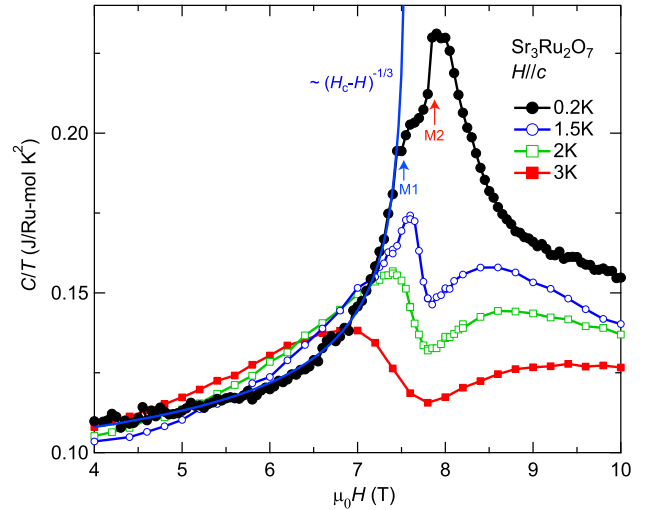

FIG. 2. Specific heat divided by temperature of $Sr_3Ru_2O_7$ as a function of magnetic field applied parallel to c axis at different constant temperatures. The solid blue line indicates $C/T = \alpha/[\mu_0(H_c - H)]^{1/3} + \gamma$ with $\alpha = (0.073 \pm 0.002)$ J/ Ru- mol $K^2 T^{1/3}$, $\mu_0 H_c = 7.57(4)$ T   and $\gamma = 0.058(1)$ J/ Ru-mol K^2, in accordance with a two-dimensional metamagnetic QCEP [3,24].

coefficient, which has a substantial noncritical background, Γ_H is more sensitive to quantum criticality because of a negligibly small noncritical contribution.

Figure 3 shows an isothermal scan of the magnetic Grüneisen parameter at 0.2 K. $\Gamma_H(H)$ increases by more than a factor of 10 in between 6 to 7.5 T. For any field-tuned QCP, the magnetic Grüneisen parameter displays a generic $1/h$ divergence [17]. Thus, the inverse of the Grüneisen parameter vs field must follow a linear dependence and crosses zero at the critical field. As shown in the inset of Fig. 3, this universal dependence is indeed observed, yielding a critical field very close to H_{M1}, which confirms our heat capacity analysis.

At fields beyond H_{M1}, a cascade of further sign changes and anomalies is found in $\Gamma_H(H)$. They are associated with metamagnetic transitions $M2$ and $M3$ and, respectively, the SDW phases A and B [12,15], as well as (see the green arrows) an anomaly labeled "C" in the phase diagram of Fig. 1, whose magnetic Grüneisen parameter signature is discussed in the Supplemental Material [14].

Each zero crossing of $\Gamma_H(H)$ from negative to positive with increasing field indicates an entropy accumulation which arises either above a QCP or at the boundary of an ordered phase. Although the behavior is very complex, it is qualitatively similar to the field dependence of the low-temperature thermal expansion coefficient [11]. A simpler field dependence with only one sign change of $\Gamma_H(H)$ related to $M2$ is found at elevated temperatures above 1 K [14]. There, the thermodynamic properties are mostly influenced by QCEP2 (cf. Fig. 1).
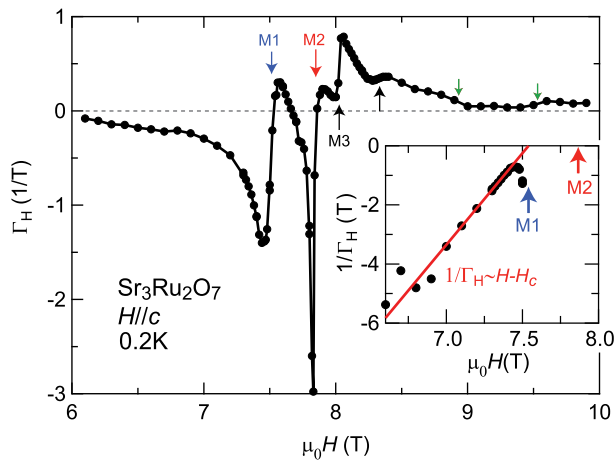
In addition to isothermal measurements, we also study the temperature dependence of Γ_H at various fields, cf. Fig. 4. At $T > 1$ K, all curves below H_{M2} show a negative Γ_H, while it is positive for $H > H_{M2}$. Since $\Gamma_H = -(dM/dT)/C$, where the heat capacity $C > 0$, this reflects the change of sign in the temperature dependence of the magnetization associated with metamagnetism (ordinary paramagnetic behavior below H_{M2} and field polarized behavior above H_{M2}). The overall symmetric behavior of $\Gamma_H(T)$ with respect to the critical field of QCEP2 is reflecting the Ising symmetry of critical metamagnetic fluctuations [24]. Upon cooling, $|\Gamma_H|$ increases within the critical regime of QCEP2 and passes a maximum upon entering the low-temperature FL state, as seen, e.g., for the 9 T data in Fig. 4. Transitions to phases A and B lead to distinct anomalies indicated by arrows. Particularly interesting behavior is found at 7.5 T where, upon cooling, $\Gamma_H(T)$ passes the minimum at 1.5 K, due to the FL crossover of QCEP2, but subsequently displays a negative divergence as $T \to 0$, related to the nearby QCEP1 (cf. Fig. 1).

We now turn to a quantitative comparison of our data with the theory of metamagnetic quantum criticality [3,24]. The latter predicts $\Gamma_H h \sim h^2/T^{(4+2d)/3}$ in the quantum critical and $\Gamma_H h = (3 - d)/3$ in FL regime, where d denotes the dimensionality and $h = \mu_0(H - H_c)$. This leads to universal scaling in a plot of $\Gamma_H h$ vs h^2/T^ϵ, where $\epsilon = (4 + 2d)/3 = 8/3$ for $d = 2$. Respective scaling behavior of our data is shown in Fig. 5. Here we fixed the critical field to 7.845 T [11], which is the position of QCEP2. The data collapse over several orders of magnitude, similar as previously found for thermal expansion [11], proves quantum critical behavior and indicates the applicability of the itinerant theory. However, a close inspection provides further information [14]. First, for
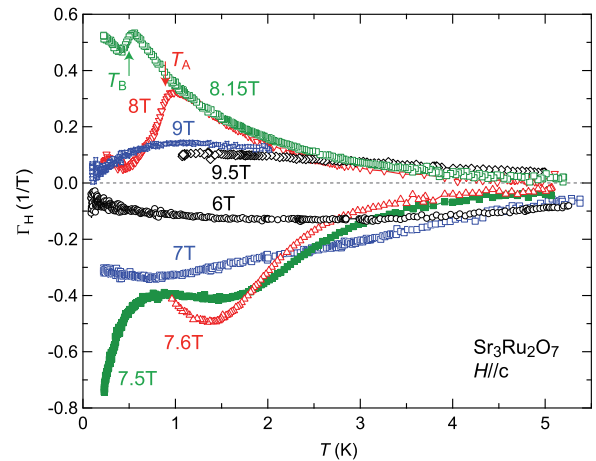

FIG. 3. Magnetic field dependence of the magnetic Grüneisen parameter Γ_H at 0.2 K of $Sr_3Ru_2O_7$. The field is applied parallel to the c axis. Arrows at $\mu_0 H_{M1} = 7.5$ T, $\mu_0 H_{M2} = 7.85$ T, and $\mu_0 H_{M3} = 8.0$ T indicate metamagnetic anomalies. The black arrow at 8.3 T marks the anomaly related to the SDW-B phase [12,15]. Green arrows indicate anomalies which correspond to open circles in Fig. 1, enclosing an anomalous regime "C". The inset shows a plot of $1/\Gamma_H$ vs $\mu_0 H$. The solid red line represents a linear fit, $1/\Gamma_H = -\mu_0(H - H_c)/G_r$ with $G_r = -0.17(1)$ and $\mu_0 H_c = 7.51(2)$ T.

FIG. 4. Magnetic Grüneisen parameter Γ_H of $Sr_3Ru_2O_7$ as a function of temperature at different magnetic fields, applied parallel to the c axis. The red and green arrows indicate the transitions to the spin-density-wave phases A and B [12].
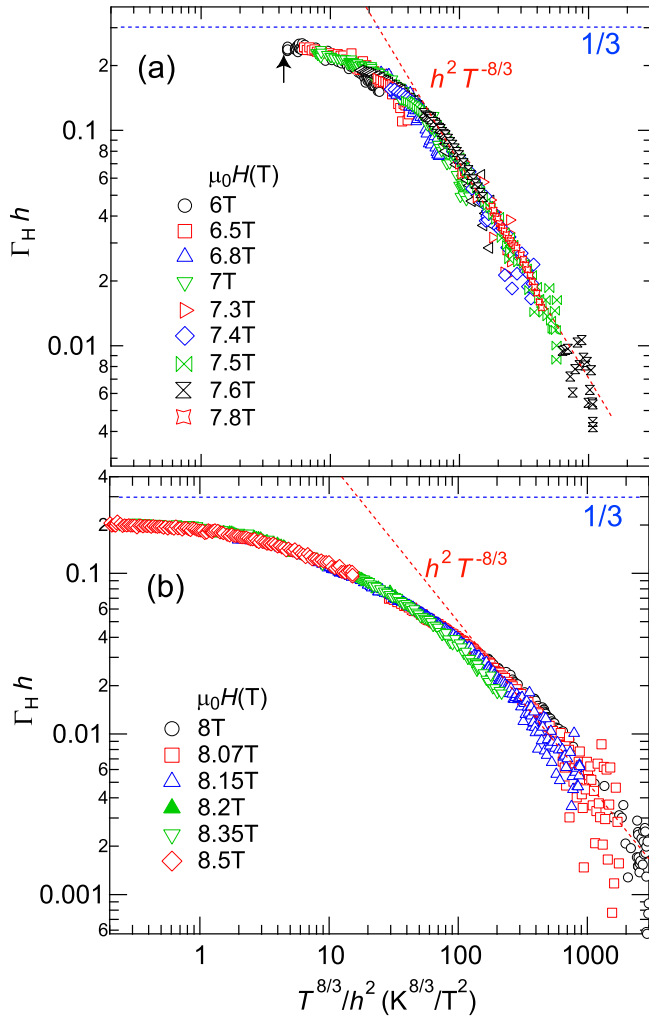
FIG. 5.   Metamagnetic quantum critical scaling of the magnetic Grüneisen parameter in $Sr_3Ru_2O_7$. The y axis displays $\Gamma_H h$, while the x axis shows $T^{8/3}/h^2$, with $h = \mu_0(H - H_{c2})$ and the critical field $\mu_0 H_{c2} = 7.845$ T [11]. Panels (a) and (b) display regimes below and above the critical field. Red and blue dotted lines indicate predicted asymptotic quantum critical and FL behavior for a $d = 2$ metamagnetic QCEP [24]. In panel (a), data on the left of the black arrow have been excluded (for failed scaling, see Supplemental Material [14]).

fields below H_{M2}, scaling is cut off near the crossover to the FL regime. This could be associated with the influence of QCEP1, as discussed above. Second, for fields $H > H_{M2}$ the data within the FL regime approach a saturation of $\Gamma_H h \approx 0.2$, which is smaller than the value $1/3$ predicted for a QCEP with dimensionality $d = 2$ [24] and may indicate that the effective dimensionality slightly increases at large fields. The value of 0.2 would correspond to $d_{\mathrm{eff}} = 2.4$. Metamagnetism in $Sr_3Ru_2O_7$ is supposed to arise from van Hove singularities near the Fermi level [26]. A change of the de Haas–van Alphen frequencies near 8 T has been ascribed to magnetic breakdown [27]. This could explain the increase of the effective dimensionality of critical fluctuations, deduced from our scaling analysis.

The different regimes where the magnetic Grüneisen parameter displays scaling with respect to QCEP 1 and QCEP2 are indicated in Fig. 1. In between both regimes neither scaling works, because criticality from both instabilities is adding up (see Supplemental Material [14]). Next, we discuss the influence of the ordered phases A and B. In the approach of these phase transitions, Γ_H data deviate from the expected quantum critical scaling. This could be naturally explained by additional contributions to the free energy arising from classical critical behavior. Furthermore, there is an anomalous depression of Γ_H at 9 T below 1 K (cf. Fig. 4), which could not be accounted for by the scaling due to QCEP2. The magnetic field dependence of $\Gamma_H(T)$ (Fig. 3, see also Supplemental Material [14]) indicates low-temperature anomalies in this field regime, labeled C in the phase diagram (Fig. 1). Since heat capacity does not show an anomaly these are rather weak thermodynamic signatures for phase formation. The fields where these anomalies are observed are temperature dependent. Thus, it is unlikely, that these anomalies originate from low frequency quantum oscillations [8].

Our measurements of the magnetic Grüneisen parameter and specific heat coefficient establish the existence of two itinerant metamagnetic QCEPs in bilayer strontium ruthenate $Sr_3Ru_2O_7$ for magnetic fields applied parallel to the c direction. QCEP1 appears at a metamagnetic crossover near 7.5 T while QCEP2, which has already previously been established, is located at 7.845 T. The phase diagram shown in Fig. 1 indicates the scaling regimes QC1 and QC2 determined from the magnetic Grüneisen parameter behavior (see also Supplemental Material [14]). While QC2 is largely extended at elevated temperatures, QC1 is confined to a narrow regimes close to QCEP1. In between these scaling regimes, there exists a range in phase space, in which scaling fails due to the superposition of criticality from both instabilities. The phase diagram is even richer and contains also two SDW phases A and B [12] and some anomalous yet unidentified regime labeled C. Likely, the observed complexity is related to the complicated electronic structure of this material [26]. The Fermi surface contains several pockets that could give rise to nesting and sheets near a van Hove singularity. From a general perspective, multiple quantum criticality may cause anomalous behaviors in different material classes, including heavy fermions and high-T_c superconductors. The Grüneisen parameter is ideally suited to disentangle multiple quantum criticality.

Note added in proof—The existence of a QCEP at $\mu_0 H_{M1}$ has most recently also been concluded from heat capacity and (non-adiabatic) magnetocaloric effect measurements [28].

[1] S. Sachdev, *Quantum Phase Transitions* (Cambridge University Press, Cambridge, UK, 1999).

[2] P. Gegenwart, Q. Si, and F. Steglich, Nat. Phys. **4**, 186 (2008).

[3] A. J. Millis, A. J. Schofield, G. G. Lonzarich, and S. A. Grigera, Phys. Rev. Lett. **88**, 217204 (2002).

[4] R. Daou, C. Bergemann, and S. R. Julian, Phys. Rev. Lett. **96**, 026401 (2006).

[5] F. Weickert, M. Brando, F. Steglich, P. Gegenwart, and M. Garst, Phys. Rev. B **81**, 134438 (2010).

[6] D. Aoki, T. Combier, V. Taufour, T. D. Matsuda, G. Knebel, H. Kotegawa, and J. Flouquet, J. Phys. Soc. Jpn. **80**, 094711 (2011).

[7] S. A. Grigera, R. A. Borzi, A. P. Mackenzie, S. R. Julian, R. S. Perry, and Y. Maeno, Phys. Rev. B **67**, 214427 (2003).

[8] A. W. Rost, R. S. Perry, J.-F. Mercure, A. P. Mackenzie, and S. A. Grigera, Science **325**, 1360 (2009).

[9] R. S. Perry, K. Kitagawa, S. A. Grigera, R. A. Borzi, A. P. Mackenzie, K. Ishida, and Y. Maeno, Phys. Rev. Lett. **92**, 166602 (2004).

[10] S. A. Grigera, P. Gegenwart, R. A. Borzi, F. Weickert, A. J. Schofield, R. S. Perry, T. Tayama, T. Sakakibara, Y. Maeno, A. G. Green, and A. P. Mackenzie, Science **306**, 1154 (2004).

[11] P. Gegenwart, F. Weickert, M. Garst, R. S. Perry, and Y. Maeno, Phys. Rev. Lett. **96**, 136402 (2006).

[12] C. Lester, S. Ramos, R. S. Perry, T. P. Croft, R. I. Bewley, T. Guidi, P. Manuel, D. D. Khalyavin, E. M. Forgan, and S. M. Hayden, Nat. Mater. **14**, 373 (2015).

[13] R. A. Borzi, S. A. Grigera, J. Farrell, R. S. Perry, S. J. S. Lister, S. L. Lee, D. A. Tennant, Y. Maeno, and A. P. Mackenzie, Science **315**, 214 (2007).

[14] See Supplemental Material at http://link.aps.org/supplemental/10.1103/PhysRevLett.116.226402, for more details on the field dependences of the specific heat and magnetic Grüneisen parameter, as well as quantum critical scaling.

[15] C. Stingl, R. S. Perry, Y. Maeno, and P. Gegenwart, Phys. Status Solidi (b) **250**, 450 (2013).

[16] A. W. Rost, A. M. Berridge, R. S. Perry, J.-F. Mercure, S. A. Grigera, and A. P. Mackenzie, Phys. Status Solidi (b) **247**, 513 (2010).

[17] L. Zhu, M. Garst, A. Rosch, and Q. Si, Phys. Rev. Lett. **91**, 066404 (2003).

[18] M. Garst and A. Rosch, Phys. Rev. B **72**, 205129 (2005).

[19] Y. Tokiwa and P. Gegenwart, Rev. Sci. Instrum. **82**, 013905 (2011).

[20] Y. Tokiwa, T. Radu, C. Geibel, F. Steglich, and P. Gegenwart, Phys. Rev. Lett. **102**, 066401 (2009).

[21] Y. Tokiwa, E. D. Bauer, and P. Gegenwart, Phys. Rev. Lett. **111**, 107003 (2013).

[22] Y. Tokiwa, M. Garst, P. Gegenwart, S. L. Bud'ko, and P. C. Canfield, Phys. Rev. Lett. **111**, 116401 (2013).

[23] R. S. Perry and Y. Maeno, J. Cryst. Growth **271**, 134 (2004).

[24] M. Zacharias and M. Garst, Phys. Rev. B **87**, 075119 (2013).

[25] H. Aoki, M. Takashita, N. Kimura, T. Terashima, S. Uji, T. Matsumoto, and Y. Ōnuki, J. Phys. Soc. Jpn. **70**, 774 (2001).

[26] A. Tamai, M. P. Allan, J. F. Mercure, W. Meevasana, R. Dunkel, D. H. Lu, R. S. Perry, A. P. Mackenzie, D. J. Singh, Z.-X. Shen, and F. Baumberger, Phys. Rev. Lett. **101**, 026407 (2008).

[27] J.-F. Mercure, A. W. Rost, E. C. T. O'Farrell, S. K. Goh, R. S. Perry, M. L. Sutherland, S. A. Grigera, R. A. Borzi, P. Gegenwart, A. S. Gibbs, and A. P. Mackenzie, Phys. Rev. B **81**, 235103 (2010).

[28] D. Sun, A. Rost, R. Perry, A. P. Mackenzie, and M. Brando, arXiv:1605.00396.